*Archives of Hydro-Engineering and Environmental Mechanics*
Vol. 52 (2005), No. 2, pp. 89–110


# A Method for Determination of Flow at the Plane Horizontal Interface, Separating Streams of Two Different Fluids

**Włodzimierz J. Prosnak, Paweł P. Cześnik**

Institute of Oceanology, Polish Academy of Sciences,
ul. Powstańców Warszawy 55, 81-712 Sopot, Poland, e-mail: czesiek@iopan.gda.pl

(Received February 14, 2005; revised March 09, 2005)

**Abstract**

The paper deals with the theoretical investigation of the phenomenon, which consists in generation – by wind – of the movement of water, the bodies of air and of water being separated by a horizontal, plane interface, which is identical with the free surface of water. A set of assumptions defining a *physical model* of the phenomenon, borrowed from Lock (1951), is introduced, as well as the *mathematical description* of this model. It reduces to a composite ordinary differential problem, containing two non-linear equations of the third order, which have to satisfy some boundary conditions.

A *novel method* of solution of the differential problem just mentioned is presented in the paper. In the method use is made of *exact formulae* for coefficients of series representing the solution. The method seems to be competitive with the one given in the paper by Lock (1951).

**Key words**: interface, almost parallel streams of two fluids, boundary layers, ordinary differential equations, asymptotic and matching conditions.

## 1. Introduction

The composite differential problem mentioned in the former Section will be derived, basing essentially on the paper by Lock (1951).

### 1.1. Fundamental Assumptions

The two fluids taken into account in the present considerations, are assumed as incompressible, and viscous, both properties being constant:

$$\rho_a = \text{const}, \quad \mu_a = \text{const}, \quad \rho_w = \text{const}, \quad \mu_w = \text{const}. \tag{1}$$

The symbols $\rho$ and $\mu$ stand for density, and dynamical viscosity, respectively Analogically, the indices $a$ and $w$ refer to *air* and *water*.

The domain of solution consists of a plane, wherein a rectangular system of coordinates $x$, $y$ is introduced, oriented with respect to the gravity field:

$$\vec{g} = \text{const}, \tag{2}$$

as shown in Fig. 1. Namely, the axes $x$, $y$ are perpendicular, and parallel to $\vec{g}$, respectively.

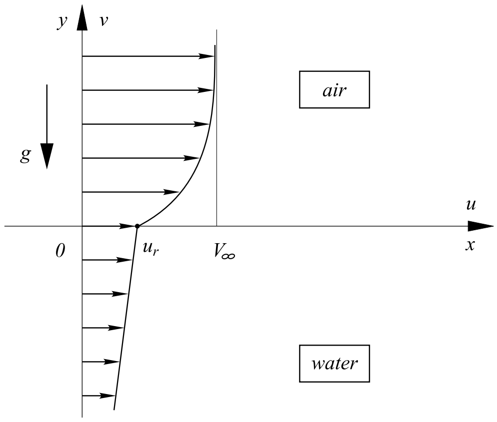


**Fig. 1.** Velocity distribution in vicinity of the interface between air and water

Furthermore, it is assumed that the $x$-axis separates the $x$, $y$ plane into two sub-domains:

$$y \geq 0, \tag{3a}$$

$$y \leq 0, \tag{3b}$$

each fluid occupying just one of the sub-domains. More exactly, air occupies the "upper" sub-domain (3a), and water – the remaining one (3b). Consequently, no waves appear on the interface, separating the fluids.

The problem to be investigated in the paper consists in *determination of the velocity fields* in both sub-domains, the fields being defined by means of the rectangular velocity components:

$$u_a = u_a(x, y), \quad v_a = v_a(x, y), \tag{4a}$$

$$u_w = u_w(x, y), \quad v_w = v_w(x, y). \tag{4b}$$

These components and their derivatives have to satisfy boundary conditions of two kinds. Namely, the *asymptotic* conditions describe behaviour of fluids at infinite distances of the interface:

$$\lim_{y\to+\infty} u_a(x,y) = V_\infty, \quad \lim_{y\to+\infty} v_a(x,y) = 0, \tag{5a}$$

$$\lim_{y\to-\infty} u_w(x,y) = 0, \quad \lim_{y\to-\infty} v_w(x,y) = 0, \tag{5b}$$

the symbol $V_\infty$ being explained by means of Fig. 1. On the other hand, the *conditions of compatibility* follow from the requirement that – on every point of the interface – the velocity of both flows and the tangential stresses must be equal:

$$u_a(x,0) = u_w(x,0) = u_r, \tag{5c}$$

$$\mu_a \left.\frac{\partial u_a}{\partial y}\right|_{y=0} = \mu_w \left.\frac{\partial u_w}{\partial y}\right|_{y=0}, \tag{5d}$$

the symbol $u_r$ denoting velocity at the interface; see the jump of the gradient of the velocity component $u$ in Fig. 1.

Finally, it is assumed, that flow of both fluids is governed by Navier-Stokes equations.

### 1.2. Possibility of Application of Poiseuille's Flows

One of the important results of Theoretical Fluid Mechanics, referred to as the plane Poiseuille flow, should be recalled here. Its generalised form is shown in Fig. 2, where the applied symbols are self-evident. It should be added, perhaps, that the domain of solution is defined, as

$$0 \le y \le h, \tag{6}$$

that the "walls" of such a domain, forming an infinite "channel", are impermeable, and all the streamlines are *parallel* to the $x$-axis. The velocity components of the walls: $U_0$, $U_h$ are given, as is width $h$ of the channel.

The flow is assumed to be steady and plane; moreover – it is governed by the system of Navier-Stokes equations in the following form:

$$\left.\begin{array}{l} u_x + v_y = 0, \\ \rho\left(uu_x + vu_y\right) = -p_x + \mu\left(u_{xx} + u_{yy}\right), \\ \rho\left(uv_x + vv_y\right) = -p_y + \mu\left(v_{xx} + v_{yy}\right), \end{array}\right\} \tag{7a}$$

where the symbols

$$u, v, p, \rho, \mu \tag{7b}$$

denote velocity components, pressure, density and viscosity, respectively.

The assumption concerning the velocity field:

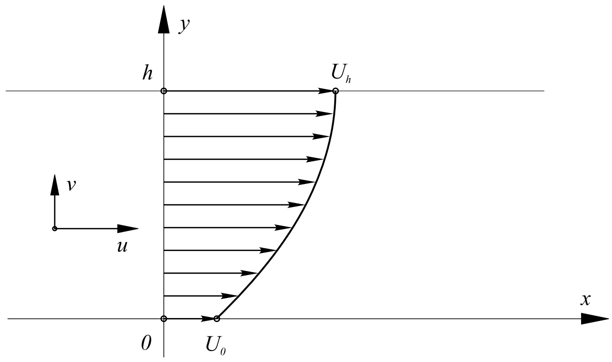


**Fig. 2.** Viscous, plane and steady flow between parallel "walls" moving with given velocities

$$v(x, y) = 0, \tag{7c}$$

allows to obtain the solution in the form of *exact* formulae. Namely, by virtue of (7c) the following results can be drawn:

$$u = u(y), \tag{8a}$$

$$p = p(x), \tag{8b}$$

$$p_x = \mu u_{yy}. \tag{8c}$$

Next, substitution of the following conditions

$$p(0) = p_0, \quad u(0) = U_0, \quad u(h) = U_h \tag{8d}$$

into (7a), yields the well known *exact solution*:

$$p(x) = p_0 + Kx, \tag{9a}$$

$$u(y) = \frac{1}{\mu}\left(\frac{1}{2}Ky^2 + C_0 y + C_1\right), \tag{9b}$$

where the newly introduced constants have the following meaning:

$$C_0 = \mu(U_h - U_0)/h - Kh/2, \tag{9c}$$

$$C_1 = \mu U_0, \tag{9d}$$

$$K = \frac{dp}{dx} = \text{const}. \tag{9e}$$

As already mentioned in this Section, the flow described by the formulae (9) is usually referred to as the *plane Poiseuille flow*.

Now let us adopt this flow to the requirements posed by the composite phenomenon presented in Fig. 1. Realisation of this idea is explained in Fig. 3, where each of the combined flows is represented by the solution (9) with proper values of the constants (9c)–(9e).

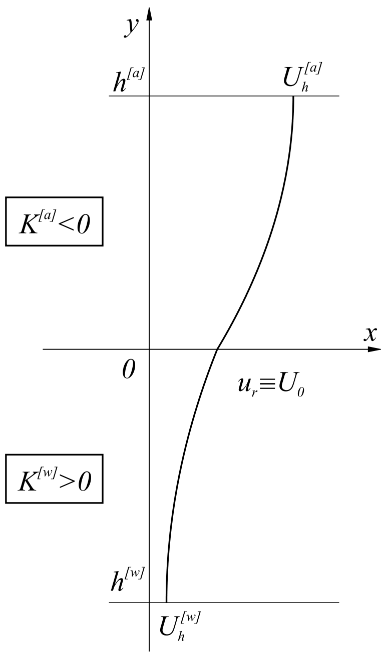


**Fig. 3.** On incompatibility of two Poiseuille flows with different viscosities

We have checked the idea on a number of examples, collected in an internal report (Prosnak, Cześnik 2003). Unfortunately, the general conclusion turned out to be **negative**. Namely, *discontinuity* of pressure on the interface occurs in the flow, which is incompatible with the fundamental physical property of the interface.

### 1.3. Combination of Two Boundary Layers. Selfsimilarity

The composite model of the flow introduced by Lock (1951) can be illustrated also by Fig. 3: the general scheme of the velocity fields remains the same. However, instead of the Poiseuille flows, discussed in the former Subsection, two special boundary layers appear in this case.

The upper layer is almost identical with the one generated by uniform stream on a flat plate, which we will refer to as the *Blasius solution* (Prandtl 1944, Prosnak, Cześnik 2003). The flow in such a boundary layer is governed by so-called Prandtl's equations, representing a simplified form of the Navier-Stokes' ones. In the system of coordinates shown in Fig. 2 they can be written as:

$$u_x + v_y = 0, \tag{10a}$$

$$u u_x + v u_y = \nu\, u_{yy}, \tag{10b}$$

the indices referring to the sub-domain (3a) being omitted, and

$$\nu = \frac{\mu}{\rho} \tag{10c}$$

denoting the kinematic viscosity.

The important property of such a boundary layer concerns the constancy of pressure:

$$p\,(x, y) = \text{const}, \tag{10d}$$

so that the "obstacle" for combination of two flows does not occur here at all. The boundary condition for the asymptotic behaviour of the velocity field says:

$$\lim_{y\to\infty} u\,(x, y) = V_\infty. \tag{10e}$$

On the interface, obviously, the velocity components have to satisfy the following conditions:

$$u\,(x, 0) = u_r, \tag{10f}$$

$$v\,(x, 0) = 0, \tag{10g}$$

the right-hand side in (10f) denoting velocity component on the interface – see Figs. 1 and 3.

Leaving aside the analogous description of the second boundary layer, the one occupying the "lower" sub-domain (3b), we shall transform the partial differential equations presented so far in this Subsection, onto ordinary ones.

Following Lock (1951), we will introduce the *stream function*:

$$\Psi = \Psi\,(x, y)\,, \tag{11a}$$

defined by the velocity components:

$$u = \frac{\partial \Psi}{\partial y}, \quad v = -\frac{\partial \Psi}{\partial x}. \tag{11b}$$

Next, using selfsimilarity, we introduce a new independent variable:

$$\eta = \left( \frac{V_\infty}{\nu \cdot x} \right)^{\frac{1}{2}} y, \tag{11c}$$

and a new unknown function

$$f = f(\eta). \tag{11d}$$

Consequently, the new and the old functions are interconnected by means of the following expressions:

$$\Psi = (\nu V_\infty x)^{\frac{1}{2}} \cdot f(\eta), \tag{11e}$$

$$u = V_\infty f'(\eta), \tag{11f}$$

$$v = \frac{1}{2} \left( \frac{V_\infty \nu}{x} \right)^{\frac{1}{2}} \left[ \eta \cdot f'(\eta) - f(\eta) \right], \tag{11g}$$

$$\frac{\partial u}{\partial y} = V_\infty \left( \frac{V_\infty}{\nu x} \right)^{\frac{1}{2}} \cdot f''(\eta), \tag{11h}$$

as well as by the sought-for ordinary equation:

$$f''' + \frac{1}{2} f f'' = 0, \tag{11i}$$

stemming from (10a), (10b).

## 2. The Composite Problem

The Section contains the formulation of two differential equations, describing flows in the sub-domains (3a) and (3b), as well as suitable conditions. Ideas concerning the solution of these two problems and matching of their solutions are also presented.

### 2.1. The Differential Problem in the Sub-Domain Occupied by Air

The problem consists of two elements:

– the equation:

$$f_a''' + \frac{1}{2} f_a f_a'' = 0, \quad f_a = f_a(\eta), \quad \eta \equiv \eta_a, \quad \eta \geq 0, \tag{12a}$$

– and boundary conditions:

$$f_a(0) = 0, \tag{12b}$$

$$f_a'(0) = c_{a1}, \quad c_{a1} = \frac{u_r}{V_\infty}, \tag{12c}$$

$$\lim_{\eta\to\infty} f_a'(\eta) = 1. \tag{12d}$$

### 2.2. The Differential Problem in the Sub-Domain Occupied by Water

The problem consists – analogically as the previous one – of:

– the equation:

$$f_w''' + \frac{1}{2} f_w f_w'' = 0, \quad f_w = f_w(\eta), \quad \eta \equiv \eta_w, \quad \eta \le 0, \tag{13a}$$

– and boundary conditions:

$$f_w(0) = 0, \tag{13b}$$

$$f_w'(0) = c_{w1}, \quad c_{w1} = \frac{u_r}{V_\infty}, \tag{13c}$$

$$\lim_{\eta\to-\infty} f_w'(\eta) = 0. \tag{13d}$$

### 2.3. The Compatibility Conditions

The streams of air (12) and water (13) have to satisfy some compatibility conditions on the interface. These conditions express equality of velocities and stresses on this plane, and can be formulated as follows.

As it stems from (12c) and (13c) the equality of **non-dimensional** velocities (11f) of the two fluids at the interface can be expressed as:

$$c_{a1} = c_{w1} = \text{const}, \quad \text{const} = c_1, \tag{14a}$$

the newly-introduced symbol $c_1$ denoting the common velocity. In Fig. 1 the **dimensional** common velocity is denoted as $u_r$. Moreover – as can be seen in Fig. 1 – the common velocity must satisfy the condition:

$$0 < u_r < V_\infty$$

in dimensional values, or the condition:

$$0 < c_1 < 1 \tag{14b}$$

in non-dimensional ones.

Equality of tangential, dimensional stresses at the interface can be expressed as

$$\mu_a \frac{\partial u_a}{\partial y}\bigg|_0 = \mu_w \frac{\partial u_w}{\partial y}\bigg|_0 \tag{14c}$$

– before application of the transformation following selfsimilarity. The condition (14c) yields

$$\mu_a V_\infty \left(\frac{V_\infty}{\nu_a x}\right)^{\frac{1}{2}} f_a''(0) = \mu_w V_\infty \left(\frac{V_\infty}{\nu_w x}\right)^{\frac{1}{2}} f_w''(0)\,,$$

as the result of the transformation. After introduction of the three auxiliary symbols:

$$\left.\begin{aligned} c_{a2} &= f_a''(0)\,, \\ c_{w2} &= f_w''(0)\,, \end{aligned}\right\} \tag{14d}$$

$$k_{\rho\mu} = \left(\frac{\rho_a \mu_a}{\rho_w \mu_w}\right)^{\frac{1}{2}} \tag{14e}$$

the second compatibility condition (14c) can be rewritten as:

$$k_{\rho\mu}\, c_{a2} = c_{w2}, \tag{14f}$$

where the symbol $k_{\rho\mu}$ from (14e) denotes the constant, characterising the two fluids.

Therefore, the formula for the error of the approximation of the unknown $c_1$ can be assumed as:

$$e_r = c_{w2} - k_{\rho\mu}\, c_{a2}. \tag{14g}$$

It depends on the second derivatives (14d) of the velocity distributions at the interface.

### 2.4. Plan for Solution of the Composite Problem

The three former Subsections lead, in the natural manner, to the plan of solution of the composite differential problem, the plan being illustrated by the block diagram, presented in Fig. 4.

It should be clearly seen, that the solution to the problem consists in determination of the non-dimensional value $c_1$ of the “common” velocity of both fluids at the interface.

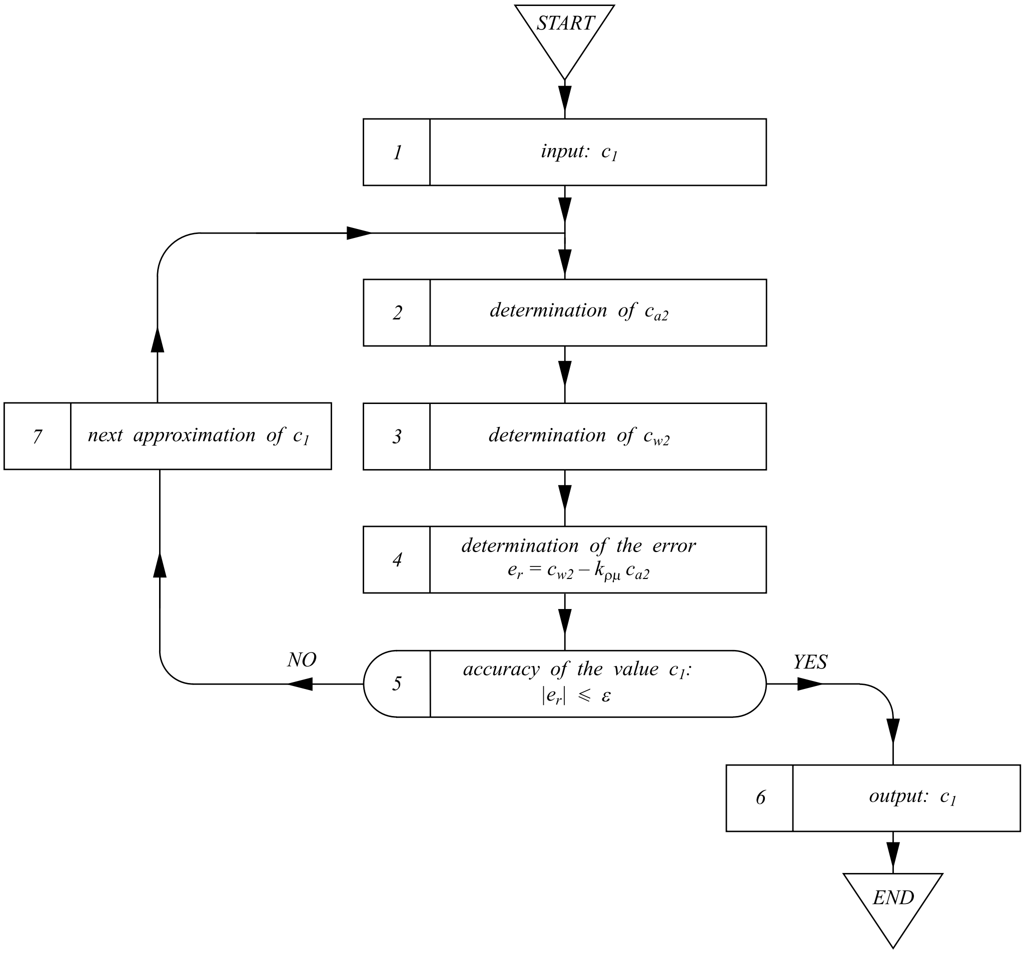


**Fig. 4.** The block diagram for the iterative process, applied for matching two viscous flows on their interface

This value is arrived at by means of an iterative process, wherein seven elements can be distinguished corresponding to the seven "boxes" of the diagram.

**Box No. 1** symbolises input of an initial value of $c_1$, which has to be guessed within the interval (14b).

**Box No. 2** refers to solution $f_a\,(\eta)$ of the differential problem (12), formulated in Subsection 2.1., the result of the solution being represented by the numerical value

$$c_{a2} = f_a\,(0)$$

of the second derivative of the function just determined – see (12a).

**Box No. 3** – analogically – refers to solution $f_w(\eta)$ of the differential problem (13), formulated in Subsection 2.2., the result being expressed by the numerical value

$$c_{w2} = f_w(0)$$

of the second derivative of the function just determined – see (13a).

**Box No. 4** indicates the calculation of error $e_r$ of the sought-for unknown $c_1$, defined by the formulae (14g).

**Box No. 5** denotes:

- checking the accuracy of the unknown $c_1$, basing on the value of the error, and
- comparing this value with the admissible one, symbolised by $\varepsilon$. If

$$|e_r| \leq \varepsilon, \tag{15a}$$

then control goes to **box No. 6**, and the iterative process is concluded. If – oppositely:

$$|e_r| > \varepsilon, \tag{15b}$$

then control goes to **box No. 7**, where a new approximation of the unknown $c_1$ has to be determined; afterwards the control returns to box No. 2.

Evaluation of consecutive values of $c_1$ is performed in two phases. During the *exploratory* one the calculations of $c_1$ are repeated, and stored, until errors belonging to two consecutive approximations $n$, $n+1$ have opposite signs:

$$(e_r)_n \cdot (e_r)_{n+1} < 0. \tag{15c}$$

During the *refinement* phase the consecutive values of $c_1$ are evaluated alternatively – by *the rule of the false position*, and by halving the distance between two "latest" values of the unknown.

The iterative process so defined turned out to be convergent, the convergence of the refinement phase being obvious. The exploratory phase can be made convergent also, simply by keeping the consecutive approximations within the interval (14b). In any case, no troubles with the iterative process appeared in our experiments.

As usual, the convergence can be accelerated, if one assumes as the first approximation of $c_1$ a value following from the already solved case, corresponding to such a value (14e), which is close to the one under consideration.

## 3. Determination of Flow in Each Particular Sub-Domain

As follows from the adopted plan of solution for the composite problem (Fig. 4), determination of flow in the "upper" sub-domain is performed quite independently of the determination of the flow in the "lower" one. The method of solution can therefore differ greatly in each case, so that – in fact – the solutions could be obtained parallelly **on a suitable computer**.

In the present paper, the methods of solving these "subproblems" are based on approximation of each unknown function by a series developed with respect to a proper "small parameter".

### 3.1. The Case of the "Upper" Sub-Domain

The differential problem concerning flow in the sub-domain occupied by air, was formulated in Subsection 2.2., the corresponding set of formulae being denoted as (12). This set will be presented in a slightly different form, wherein the subscript $a$ is omitted. It yields:

$$f = f(\eta), \quad \eta \geq 0, \tag{16a}$$

$$f''' + \frac{1}{2} f f'' = 0, \tag{16b}$$

$$f(0) = c_0 = 0, \tag{16c}$$

$$f'(0) = c_1, \quad 0 < c_1 < 1, \tag{16d}$$

$$\lim_{\eta \to +\infty} f'(\eta) = 1. \tag{16e}$$

The "small" parameter

$$\varepsilon_g = c_1 - 1 \tag{17a}$$

will now be introduced, which enables approximation of the unknown function (16a) by means of the power series:

$$\boxed{f(\eta) = (c_0 + \eta) + \sum_{t=1}^{\infty} \varepsilon_g^t f^{[t]}(\eta).} \tag{17b}$$

The symbol:

$$f^{[t]}(\eta), \quad t = 1, 2, \ldots \tag{17c}$$

denotes functional coefficients. Determination of the approximating function (17b) reduces – of course – to determination of the functional coefficients (17c). This can be done in the following manner:

1. approximation (17b) is substituted into equation (16b), which yields:

$$\sum_{t=1}^{\infty} \varepsilon_g^t \frac{d^3 f^{[t]}}{d\eta^3} + \frac{1}{2}\left[\eta + \sum_{t=1}^{\infty} \varepsilon_g^t f^{[t]}\right] \cdot \sum_{t=1}^{\infty} \varepsilon_g^t \frac{d^2 f^{[t]}}{d\eta^2} = 0, \tag{17d}$$

2. the expression so obtained is presented as the power series developed with respect to $\varepsilon_g^t$, the consecutive terms of the series, corresponding to exponents:

$$t = 1,\ 2,\ 3,\ \ldots,\ n \tag{17e}$$

appearing as:

$$\frac{d^3 f^{[1]}}{d\eta^3} + \frac{1}{2}\eta \frac{d^2 f^{[1]}}{d\eta^2} = 0, \tag{17f}$$

$$\frac{d^3 f^{[2]}}{d\eta^3} + \frac{1}{2}\eta \frac{d^2 f^{[2]}}{d\eta^2} = -\frac{1}{2} f^{[1]} \frac{d^2 f^{[1]}}{d\eta^2}, \tag{17g}$$

$$\frac{d^3 f^{[3]}}{d\eta^3} + \frac{1}{2}\eta \frac{d^2 f^{[3]}}{d\eta^2} = -\frac{1}{2}\left[ f^{[1]} \frac{d^2 f^{[2]}}{d\eta^2} + f^{[2]} \frac{d^2 f^{[1]}}{d\eta^2}\right], \tag{17h}$$

...........................................................................

$$\frac{d^3 f^{[n]}}{d\eta^3} + \frac{1}{2}\eta \frac{d^2 f^{[n]}}{d\eta^2} = -\frac{1}{2}\sum_{t=1}^{n-1} f^{[t]} \frac{d^2 f^{[n-t]}}{d\eta^2}. \tag{17i}$$

The equation (17f) for $f^{[1]}(\eta)$, provided with proper boundary conditions, can be presented as the following differential problem for the fundamental coefficient just mentioned:

$$f^{[1]'''} + \frac{1}{2}\eta \cdot f^{[1]''} = 0, \tag{18a}$$

$$f^{[1]}(0) = 0, \tag{18b}$$

$$f^{[1]'}(0) = 1, \tag{18c}$$

$$\lim_{\eta \to +\infty} \frac{df^{[1]}}{d\eta} = 0. \tag{18d}$$

The solution to this problem, or – more exactly – the unknown function $f^{[1]}(\eta)$, together with its derivatives $f^{[1]'}(\eta)$ and $f^{[1]''}(\eta)$, are drawn in Fig. 5.

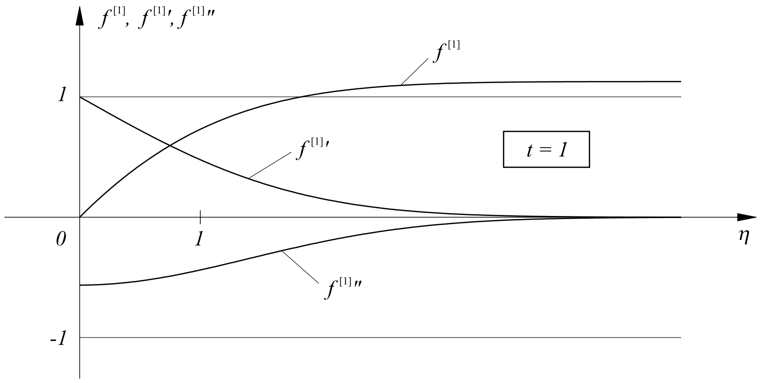


**Fig. 5.** The function $f^{[1]}$ as well as its first $f^{[1]'}$ and second $f^{[1]''}$ derivatives, exemplifying one element of the function (17b), i.e. of the velocity distribution in the "upper" sub-domain

It should be seen, that the equation (18a) is linear and can be solved exactly.

The differential problems for the functional coefficients for $t > 1$ can be presented recurrently as:

$$f^{[n]'''} + \frac{1}{2}\eta \cdot f^{[n]''} = -\frac{1}{2}\sum_{t=1}^{n-1} f^{[t]} f^{[n-t]''}, \tag{19a}$$

$$f^{[n]}(0) = 0, \tag{19b}$$

$$f^{[n]'}(0) = 0, \tag{19c}$$

$$\lim_{\eta \to +\infty} \frac{df^{[n]}}{d\eta} = 0, \ (t > 1). \tag{19d}$$

All of them are also linear, and can be solved in an exact manner.

Two further functional coefficients: for $t = 3$ and $t = 15$, are shown in Figs. 6 and 7, respectively, in order to illustrate their behaviour for increasing $t$, and their convergence.

On the other hand, Fig. 8 represents the final solution to the problem (16a)–(16e) – in the form of the function (17b) and its two derivatives.

It should be emphasised, that all the functional coefficients are expressed by exact formulae, containing truncated Tchebyshev series.

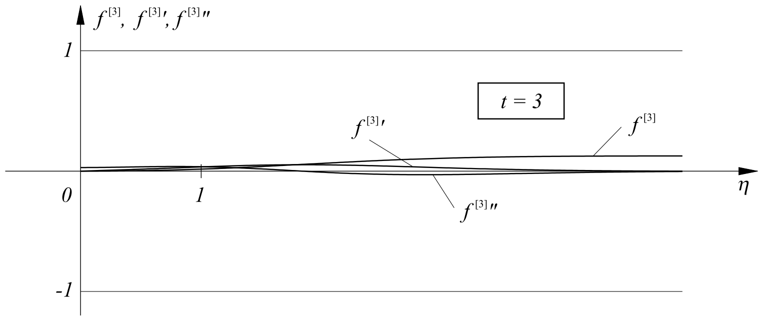


**Fig. 6.** The function $f^{[3]}$ as well as its derivatives $f^{[3]'}$ and $f^{[3]''}$, exemplifying a further element of the function (17b), i.e. of the velocity distribution in the "upper" sub-domain

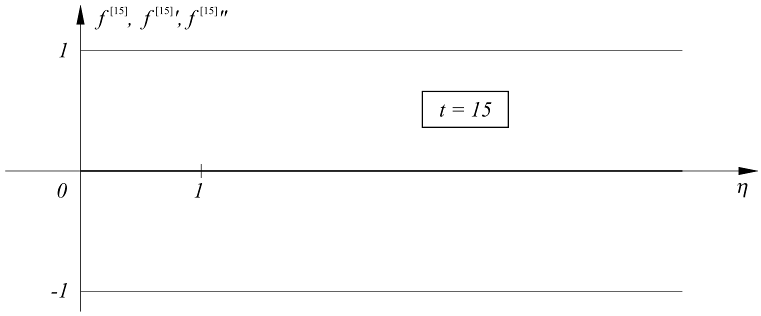


**Fig. 7.** The function $f^{[15]}$ as well as its derivatives $f^{[15]'}$ and $f^{[15]''}$, exemplifying the last element of the truncated function (17b), i.e. of the velocity distribution in the "upper" sub-domain. Note: the diagram of the function and its derivatives do not differ from the $\eta$-axis in the Fig. 7, due to the adopted scale

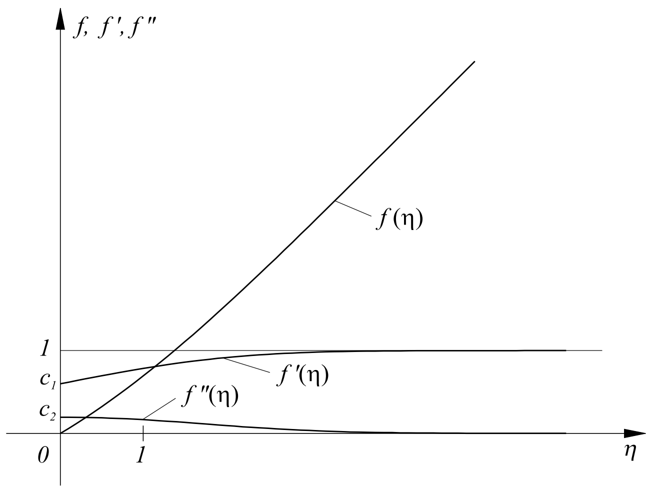


**Fig. 8.** The series (17b) truncated at the 15th term, presented together with its two derivatives

### 3.2. The Case of the "Lower" Sub-Domain

The same approach as in the former Subsection will be applied to the problem formulated in Subsection 2.3., and described by the set of formulae (13). For the sake of convenience the unknown function $f_w(\eta)$ will be now denoted as $F(\eta)$, so that the problem to be considered can be presented as follows:

$$F = F(\eta), \quad \eta \leq 0, \tag{20a}$$

$$F''' + \frac{1}{2} F F'' = 0, \tag{20b}$$

$$F(0) = 0, \tag{20c}$$

$$F'(0) = c_1, \quad 0 < c_1 < 1, \tag{20d}$$

$$\lim_{\eta \to -\infty} F'(\eta) = 0. \tag{20e}$$

Now, instead of (17a) another "small" parameter is introduced:

$$\varepsilon = c_1. \tag{20f}$$

The difference between the small parameters (20f) and (17a) causes unexpectedly large differences between the two sets of results – as will be seen.

The approximating function, analogous to (17b), now appears in the form:

$$\boxed{F(\eta) = \sum_{t=1}^{\infty} \varepsilon^t F^{[t]}(\eta),} \tag{20g}$$

where

$$F^{[t]}(\eta), \quad t = 1, 2, \ldots \tag{20h}$$

denote functional coefficients. It should be stressed, that no "special" equation appears now for any value of $t$, contrary to the former case.

In a manner similar to that in Subsection 3.1. the unknown function (20g) is now substituted into the equation (20b), and – after developing the obtained result into power series, with respect to $\varepsilon^t$ – one arrives at the following, recurrent system of equations for the functional coefficients:

$$F^{[t]'''} = -\frac{1}{2} \sum_{k=1}^{t-1} F^{[k]} \cdot F^{[t-k]''}, \quad t = 1, 2, \ldots . \tag{20i}$$

The boundary conditions for $t = 1$ appear as:

$$F^{[1]}(0) = 0, \tag{20j}$$

$$F^{[1]'}(0) = 1, \tag{20k}$$

$$F^{[1]'}(\eta_{\min}) = 0, \quad \eta_{\min} = -5, \tag{20l}$$

and the solution to this differential problem is presented in the form of three lines in Fig. 9.

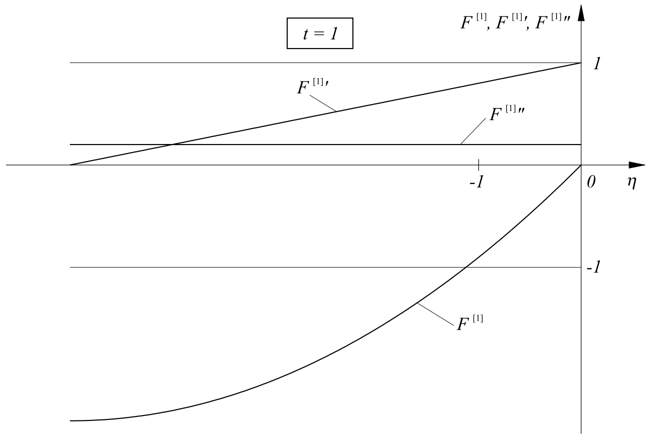


**Fig. 9.** The function $F^{[1]}$ as well as its first $F^{[1]'}$ and second $F^{[1]''}$ derivatives, exemplifying element of the function (20g), i.e. of the velocity distribution in the "lower" sub-domain

The boundary conditions are identical for all consecutive values of $t > 1$:

$$F^{[t]}(0) = 0, \tag{20m}$$

$$F^{[t]'}(0) = 0, \tag{20n}$$

$$F^{[t]'}(\eta_{\min}) = 0, \quad \eta_{\min} = -5. \tag{20o}$$

Solution for a further functional coefficient, namely $t = 3$, is presented in Fig. 10.

Results obtained in Section 3 will be discussed in the final one. Here we confine ourselves to the illustration of the solution (20g), represented as the sum of 15 terms: see Fig. 11.

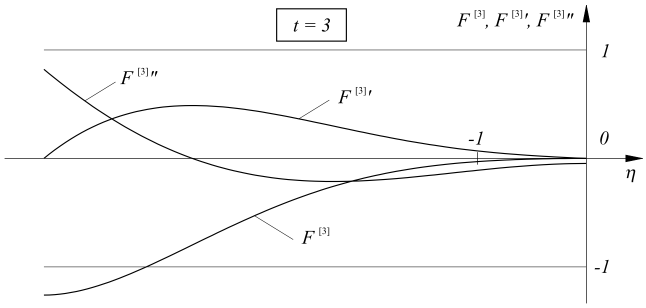


**Fig. 10.** The function $F^{[3]}$ as well as its derivatives $F^{[3]'}$ and $F^{[3]''}$, exemplifying a further element of the function (20g), i.e. of the velocity distribution in the "lower" sub-domain

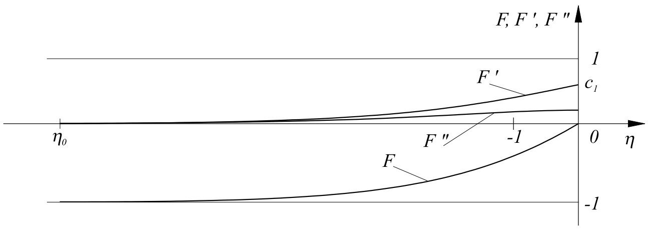


**Fig. 11.** The series (20g) truncated at the 15th term, presented together with its two derivatives

## 4. Examples of Solutions to Composite Problems

In accordance with the block diagram shown in Fig. 4, the two particular solutions (17b) and (20g) have to be matched – by the use of the compatibility condition for stresses (14f). In order to satisfy this condition, the value $c_1$ of velocity on the interface has to be determined.

Consequently, the solution of the composite problem consists of two functions:

$$f(\eta) = \eta + \sum_{t=1}^{N_a} (c_1 - 1)^t \, f^{[t]}(\eta), \quad \eta \in [0, \ \eta_{\max}], \tag{21a}$$

$$F(\eta) = \sum_{t=1}^{N_w} c_1^t F^{[t]}(\eta), \quad \eta \in [\eta_{\min}, \ 0]. \tag{21b}$$

A computer program, determining automatically the solution (21a), (21b), can be found in our internal report: Prosnak, Cześnik (2003).

An example of the solution, illustrating the functions (21a), (21b) and their derivatives, is shown in Fig. 12.

It corresponds to

$$k_{\rho\mu} = 1, \quad c_0 = 0, \quad \eta_{\max} = 5, \quad \eta_{\min} = -5. \tag{21c}$$

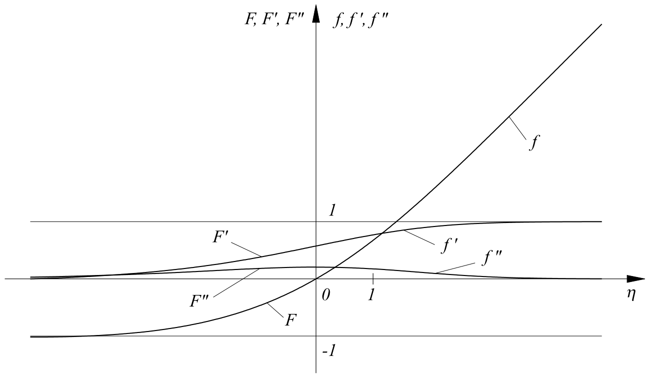


**Fig. 12.** Both functions $f(\eta)$, $F(\eta)$ matched at the interface, representing the sought for velocity distribution in the whole domain of solution (the case corresponding to $k_{\rho\mu} = 1$; see Table 1)

Selected functional coefficients of this solution have been shown in Figs. 5, 6, 7, 9 and 10. On the other hand, Figs. 8 and 11 represent the right and the left part of Fig. 12, respectively.

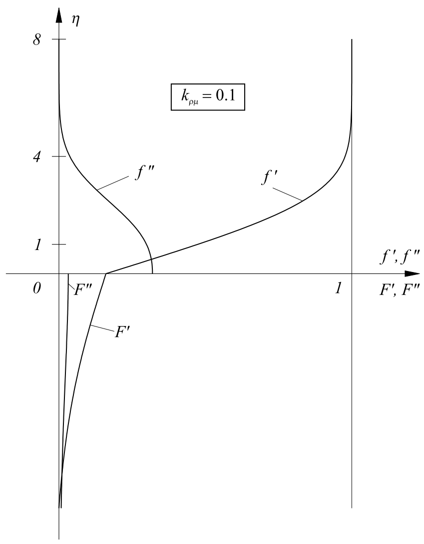


**Fig. 13.** Both functions $f(\eta)$, $F(\eta)$ matched at the interface, representing the sought for velocity distribution in the whole domain of solution (the case corresponds to $k_{\rho\mu} = 0.1$; see Table 1)

It should be noted, that the functions (21a) and (21b) are continuous – see Fig. 12. The same is true as far as their derivatives are concerned. The reason of this behaviour is obvious. The value $k_{\rho\mu} = 1$ can be interpreted as identity of both fluids with respect to density and viscosity. There is therefore no reason for discontinuities of these properties on the interface.

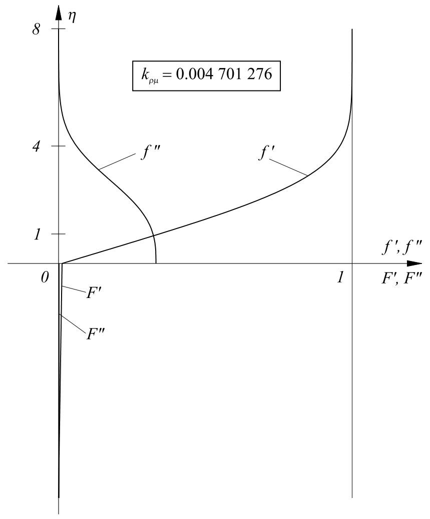


**Fig. 14.** Both functions $f(\eta)$, $F(\eta)$ matched at the interface, representing the sought for velocity distribution in the whole domain of solution (the case corresponds to the combination of air over water, i.e. to $k_{\rho\mu} = 0.004\,701\,276$; see Table 1)

Two further examples of solution to composite problems are presented in Figs. 13 and 14. They are quite analogous to Fig. 12, the only difference being, that the applied system of coordinates was borrowed from Lock (1951), which makes comparison of his results with ours fairly easy.

**Table 1.** Collection of the investigated cases

| No. | $k_{\rho\mu}$ | $c_1$ | $c_{a2}$ | $c_{w2}$ |
|---|---|---|---|---|
| 1 | 1 | 0.585 352 556 | 0.200 465 971 | 0.200 465 971 |
| 2 | 0.5 | 0.430 899 834 | 0.255 672 565 | 0.127 836 283 |
| 3 | 0.3 | 0.326 864 336 | 0.285 708 421 | 0.085 712 526 |
| 4 | 0.2 | 0.255 757 209 | 0.302 513 303 | 0.060 502 661 |
| 5 | 0.1 | 0.160 683 760 | 0.319 669 180 | 0.031 966 918 |
| 6 | 0.05 | 0.095 877 185 | 0.327 436 608 | 0.016 371 830 |
| 7 | 0.01 | 0.024 217 338 | 0.331 746 217 | 0.003 317 462 |
| 8 | 0.004 701 276 | 0.011 920 257 | 0.331 982 424 | 0.001 560 741 |
| 9 | 0.004 092 700 | 0.010 436 352 | 0.332 000 245 | 0.001 358 777 |

Final results of some further examples are collected in Table 1, demonstrating dependence of the velocity $c_1$ and the stresses $c_{a2}$, $c_{w2}$ at the interface – on values of the constant $k_{\rho\mu}$. Results Nos. 8 and 9 correspond to air and water, the difference of the results stemming from the sources, from which values of densities and viscosities have been borrowed.

## 5. Conclusions and Comments

The paper is motivated by the same needs, which occurred in connection with a problem of flow, wherein free surface of water represents an important element. We started with the study of one of the first publications concerning this element, i.e. the paper by Lock (1951). In fact, the present investigation could be alternatively entitled as:

*Lock's paper – revisited*

**The physical model** applied in his paper (1951) consists of two boundary layers, separated by a plane, horizontal interface. Therefore, the streamlines are not *exactly parallel* to the interface, and the word "parallel" appearing in the title of Lock's paper – is misleading. The same error can be found in another paper – by Lessen (1949), wherein the physical model of the phenomenon consists also of a couple of boundary layers.

**The mathematical description** of the model makes use of self-similarity of flow, this property enabling to transform all the partial derivatives and equations into ordinary ones. In consequence, the flow in each part of the solution is described by the same ordinary differential equations (12a) and (13a), representing a special form of the *Falkner-Skan* equation: (Falkner, Skan 1931, Prosnak 1961, 1962, 1969, Prosnak, Czerwińska 1995). These two flows must be matched on the interface, where the velocities of each flow and their stresses must be equal.

The differential problem consisting of two differential equations, and an iterative algorithm for their matching – is called **the composite problem** in our paper.

To solve this problem, Lock (1951) applies the well-known method of Blasius, which – we believe – does not have to be explained here. In the present paper we have used our own method (Prosnak 1961, 1962, 1969), basing on the introduction of a small parameter, which does not appear in the equation (as is usually the case), but in the boundary conditions. Each of the unknown functions, which occur in the composite problem, is approximated by power series developed with respect to the small parameter, which is different in each equation. The said approximations contain corresponding functional coefficients, which can be computed recurrently by means of exact formulae. Finally, it turns out, that the solution to the composite problem as a whole depends on the truncated Tchebyshev series.

The method presented is not difficult to program. Moreover, its ready version written in Turbo Pascal can be found in an internal report: (Prosnak, Cześnik 2003). Some other merits of the method should be mentioned, such as its accuracy, and arbitrarily extensive domains of existence $(+\eta_{\max}, -\eta_{\min})$.

Two other versions of our method of solution have been tested, *basing* on the same block diagram as the one shown in Fig. 4, but on different means for determination of the second derivatives (14d), than the one using the exact formulae, and described in Subsections 3.1 and 3.2. The alternative approaches are reported in Prosnak, Cześnik (2002a, 2002b). Being workable, they are nevertheless inferior to the one presented in this paper, and – as such – they will not be recommended – or even presented – by ourselves.

Although the revisited paper – Lock (1951) – seems to be rather ancient, having been published more than 50 years ago, the physical problem dealt with can be hardly considered as such.

Some simple considerations on a slightly different approach, basing on the Navier-Stokes equations and resembling the plane Poiseuille flow, had been discussed also – in order to indicate a possible way leading to the physical model applied by Lock (1951), and consisting of two boundary layers.

## References

Falkner V. H., Skan S. W. (1931), Some Approximate Solutions of the Boundary Layer Equations, *Phil. Mag.,* Vol. 12, p. 865.

Lessen M. (1949), *On the Stability of the Free Laminar Boundary Layer between Parallel Streams*, N.A.C.A. Tech. Note 1929.

Lock R. C. (1951), The Velocity Distribution in the Laminar Boundary Layer between Parallel Streams, *The Quarterly Journal of Mechanics and Applied Mathematics,* No. 4, 42–63.

Prandtl L. (1944), *Strömungslehre*, F. Vieweg & Sohn, Braunschweig.

Prosnak W. J. (1961), *On the Viscous Flow Near the Stagnation Point on an Interface*, Princeton University, Report 563, AFOSR 1592.

Prosnak W. J. (1962), On the Viscous Flow Near the Stagnation Point on an Interface, *Arch. Mech. Stos.,* 3/4, **14**, 505–542.

Prosnak W. J. (1969), On a Small Parameter Method for Solving Certain Selfsimilar Problems of Viscous Fows, *Bul. Ac. Pol.: Tech.,* **17**, 39–46.

Prosnak W. J., Czerwińska J. (1995), *Solution of a Boundary Problem for the Falkner-Skan Equation by Means of Discrete Methods*, Scientific Reports of the IMP – PAN in Gdańsk, 451/1407/95, (in Polish).

Prosnak W. J., Cześnik P. P. (2002a), *Determination of Flow in the Layer, Containing Horizontal Interface of Two Streams Containing Almost Parallel Streamlines, Separating Liquids of Different Viscosities and Densities, Part 1: the Shooting Method*, Internal Report No. 20 of the Laboratory of Numerical Fluid Mechanics, Institute of Oceanology, Polish Academy of Sciences, Sopot (in Polish).

Prosnak W. J., Cześnik P. P. (2002b), *Determination of Flow in the Layer, Containing Horizontal Interface of Two Streams Containing Almost Parallel Streamlines, Separating Liquids of Different Viscosities and Densities, Part 2: Small Parameter – Finite Difference Method*, Internal Report No. 21 of the Laboratory of Numerical Fluid Mechanics, Institute of Oceanology, Polish Academy of Sciences, Sopot (in Polish).

Prosnak W. J., Cześnik P. P., (2003), *Determination of Flow in the Layer, Containing Horizontal Interface of Two Streams Containing Almost Parallel Streamlines, Separating Liquids of Different Viscosities and Sensities, Part 3: Small Parameter – Analytic Method*, Internal Report No. 23 of the Laboratory of Numerical Fluid Mechanics, Institute of Oceanology, Polish Academy of Sciences, Sopot (in Polish).